CONDITION MONITORING OF MEDIUM VOLTAGE ELECTRICAL CABLES BY MEANS OF PARTIAL DISCHARGE MEASUREMENTS

H. van Jaarsveldt* and R. Gouws**

*School of Electrical, Electronic and Computer Engineering, North-West University, Private bag X6001, Post-point 288, Potchefstroom, South-Africa, 2520. *E-mail: 20569408@nwu.ac.za*
***E-mail: Rupert.Gouws@nwu.ac.za*

Abstract: The purpose of this paper is to discuss condition monitoring (CM) of medium voltage electrical cables by means of partial discharge (PD) measurements. Electrical cables are exposed to a variety of operational and environmental stressors. The stressors will lead to the degradation of the cable's insulation material and ultimately to cable failure. The premature failure of cables can cause blackouts and will have a significant effect on the safety of such a network. It is therefore crucial to constantly monitor the condition of electrical cables. The first part of this paper is focussed on fundamental theory concepts regarding CM of electrical cables as well as PD. The derivation of mathematical models for the simulation of PD is also discussed. The simulation of discharge activity is due to a single void within the insulation material of medium voltage cross-linked polyethylene (XLPE) cables. The simulations were performed in the MATLAB® Simulink® environment, in order to investigate the effects of a variety of parameters on the characteristics of the PD signal. A non-intrusive CM technique was designed for the detection of PD activity within cables. The CM technique was used to measure and analyse practical PD data. Two MATLAB® programs were designed to analyse the PD data in both the time-domain and frequency-domain.

Keywords: Condition monitoring (CM), partial discharge (PD), cross-linked polyethylene (XLPE) insulation, MATLAB® Simulink®, time- and frequency domain.

1. INTRODUCTION

Electrical networks are interconnections of expensive electrical equipment. Electrical cables are one of the most important parts of any electrical network, as it is used for the transmission of electricity between the variety of electrical equipment. Electrical cables also form an integral part in the safety of any network, as failing cables can lead to the death of employees as well as the damage of expensive equipment. Different types of medium voltage electrical cables are available, each with their own advantages and disadvantages. The type of cable to use is often influenced by the purpose and the physical environment of the cable. Cables are exposed to a variety of environmental and operational stressors which can lead to the degradation of the insulation material and ultimately to cable failure. The level of aging and degradation of electrical cables can be evaluated by means of condition monitoring (CM) techniques [1].

Partial discharge (PD) is classified as both a symptom of degradation as well as a stress mechanism of degradation and will dominate as one of the main degradation mechanisms for medium voltage electrical cables [2]. Due to this, CM techniques, which make use PD measurements, are often used to monitor the condition of electrical cables. PD is the result of localised gasses breakdowns which will occur if the conditions are suitable. A discharge is classified as partial, if the discharge doesn't completely bridge the insulation between two terminals [3].

Since the beginning of the 1990s most energy companies invested in the development of CM techniques. The process of performing CM on electrical equipment can be described as: "Condition monitoring can be defined as a technique or process of monitoring the operating characteristics of a machine in such a way that changes and trends of the monitored characteristics can be used to predict the need for maintenance before serious deterioration or breakdown occurs" [4]. CM techniques are used mainly due to the health of employees and the safe operation of electrical equipment. Any CM technique can be described as an interconnection of the following four main parts:

- Sensor.
- Fault detection.
- Data acquisition.
- Diagnosis.

The choice of sensor is influenced by the physical environment of the equipment being monitored as well as the specific technique used to monitor the equipment. Sensors are used to convert a physical quantity to an electrical signal [4]. The main objective of any CM technique is to detect electrical faults. Fault detection can be described as the process of determining whether a fault is present in equipment being monitored. The data acquisition unit of a CM technique is the link between the measuring of data and the analysis of the measured data. The main purposes of a data acquisition unit are: to amplify the measured signals, the correction of sensor failures and in some cases the conversion of measured

data from analog to digital [4]. The diagnosis of measured data is used to identify trends as well as specific degradation mechanisms [1]. The interpretation of analysed data can be seen as the most important part of any CM technique and is generally performed by a specialist.

The condition of electrical cables needs to be monitored on a regular basis in order to prevent the cables from failing prematurely and causing blackouts. The physical condition of an electrical cable can be determined by the observation, measurement and trending of condition indicators [1]. The ideal cable CM technique adheres to the following desired attributes of a CM technique [5]:

- Non-intrusive and non-destructive.
- Applicable to cable types and materials commonly used.
- Affordable and easy to perform.
- Provides trendable data.
- Capable of measuring property changes that are trendable and that can be correlated to functional performance during normal service.
- Able to identify the location of faults within the cables being tested.
- Able to detect aging and degradation before cable failure.
- Allows a well-defined end condition to be established.

It is impossible for a single technique to adhere to all of the above mentioned desired attributes. A single technique may therefore not be able to completely characterize the condition of an electrical cable. It is important to use a CM program with multiple CM techniques to successfully monitor electrical cables [5].

Electrical detection is a technique commonly used for the detection of PD within electrical cables. Electrical detection of PD can be divided into three groups [2]: 1) the measurement of individual discharge pulses, 2) measurement of total, integrated loss in the insulating material due to discharge activity and 3) the measurement of electromagnetic field effects associated with PD. The technique used to measure individual discharge pulses are commonly used as a CM technique for cables. This technique can be performed by means of a high frequency current transformer (HFCT) connected around the cable. The output of the CT is then measured by means of a digital oscilloscope or similar recording device. The use of a HFCT is a simple and affordable method to perform and also has the safety advantage of being isolated from the generally high operating voltages.

The purpose of this paper is to discuss the design and implementation of a CM technique which make use of PD measurements. The CM technique is focussed on monitoring the condition of medium voltage cables.

2. DESIGN

The purpose of this section is to discuss the design of a cable CM technique, which make use of PD measurements to analyse the condition of electrical cables. The IEEE Guide for Field Testing and Evaluation of the Insulation of Shielded Power Cable Systems will be consulted during the design process of the CM technique [6]. According to the guide PD data can be measured by means of special sensors connected to a splice or termination of the cable. The designed system makes use of a digital oscilloscope to store measured data obtained from the sensors. Designed MATLAB® programs were used to analyse the stored PD data in both the time- and frequency domain. Figure 1 shows an overview of the designed system.

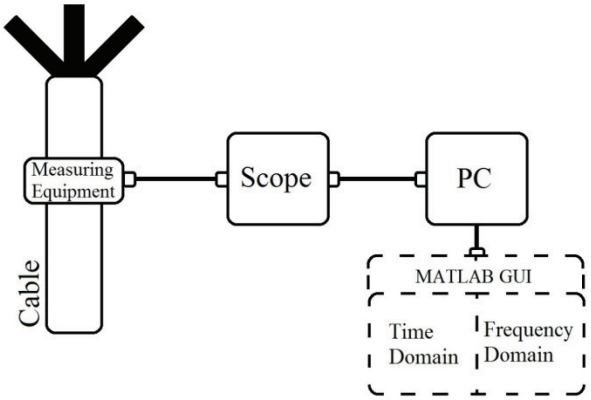

Figure 1: Overview of designed CM technique

An HFCT is used as the sensor device for the detection of PD activity. The physical construction of the HFCT is in the shape of a horseshoe and will allow the user to connect and disconnect the sensor around the cable with ease. The use of an HFCT also isolates the user from the generally high operating voltages and there is also no need for disconnections of cables being tested. The HFCT will be connected directly to a digital oscilloscope. Figure 2 (a) illustrates the commonly used split-core HFCT [7]. An HFCT with the horseshoe structure is shown in Figure 2 (B). Figure 2 illustrates the physical differences between these types of sensors and from this it can be seen that the horseshoe clamp allows for the ease of connection as well as disconnection around cables.

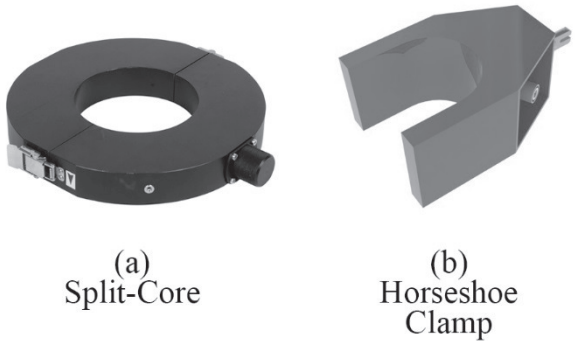

Figure 2: Two HFCT models: (a) split-core [7] and (b) Horseshoe

The system is designed to take PD measurements and store the data on a PC for analysis. The Handyscope HS5, a product of TiePie engineering, will be used as the data acquisition device. The need for a pre-amp is eliminated, due to the sufficient sensitivity of the HS5. The key specifications of the HS5 are shown in table 2.

Table 2: Handyscope HS5 specifications

Product Code	HS5-220
Max. Sampling Speed	200 Ms/s
Bandwidth	250 MHz
Resolution	14bit (0.006%), (16bit enhanced)
Memory	32 M Samples per channel
Accuracy	0.25% DC vertical, 0.1% typical

The PC is used as the device to control the system and also for storage of the recorded data. Two MATLAB® programs were designed to analyse the measured data in both the time- and frequency-domain. The time domain MATLAB® program is designed to display the measured signal in the time domain and to calculate the values for the maximum PD amplitude as well as the average PD amplitude. The time domain program is also used to determine the amount of discharges per phase and the exact position of each discharge within each phase. The results obtained from these two functions are used to perform phase resolved partial discharge (PRPD) analysis of the measured data. The functional flow diagram of these two functions is illustrated in Figure 3.

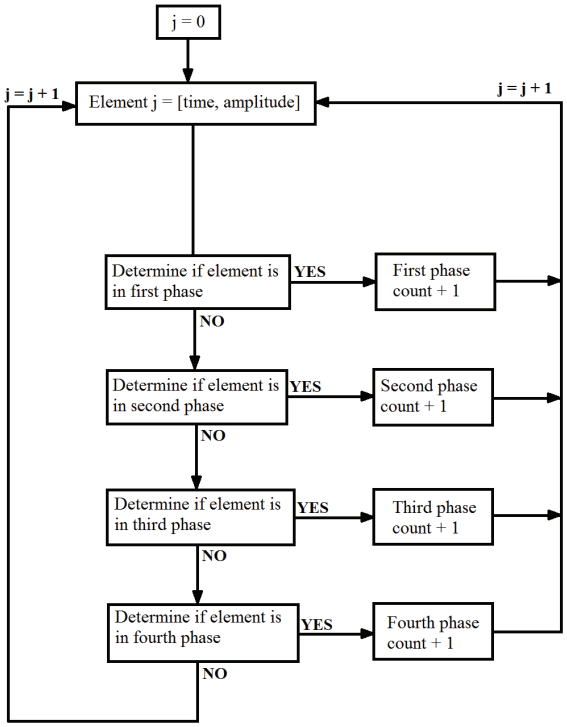

Figure 3: Functional flow diagram of source code

The functional flow illustrates that these two functions will analyse each data point individually. The stored data is in the form of a matrix, with each data point containing two elements: time and amplitude. The time element of each data point is used to determine the specific phase of the measured discharge. The function to determine the amount of discharges per phase will only determine the amount of discharge for a specific phase, as the position of each pulse is not important for this function. PRPD analysis of PD data can be used to determine the source of the discharges. This is an essential part of any CM technique, as different sources may not affect the degradation of the insulation material at the same rate.

A MATLAB® program was also designed for the purpose of analysing the measured data in the frequency domain. The transformation process is used to convert a signal from the time domain to the frequency domain and vice versa, this can also be seen as the most important concept of frequency domain analysis. A built-in fast Fourier transform (FFT) of MATLAB® is used for the transformation purposes of the CM technique. FFT functions are commonly used to convert time domain data to the frequency domain by computing the discrete Fourier transform (DFT) of the signal. The functional flow of a FFT function is shown in Figure 4.

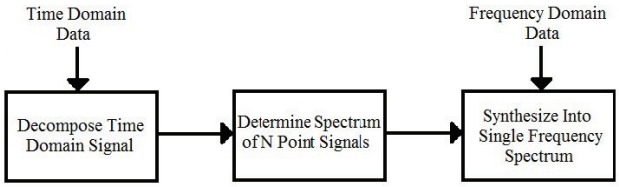

Figure 4: Functional flow diagram of an FFT function

The first step of the FFT function is to decompose an N point signal into N single point signals. This is then used to determine the spectrum of each individual point. The final step of the FFT function is to synthesize the N frequency spectra into a single frequency spectrum.

The frequency domain analysis of the measured data will be used to determine at which frequencies the discharge activity is more prolific. The FFT plot can also be used to determine the severity of PD activity as well as the location of the fault.

3. SIMULATED PARTIAL DISCHARGE RESULTS

3.1 Introduction

The purpose of this section is to discuss the derivation of mathematical models for the simulation of PD. The development of electrical models to study the behaviour of PD activity within the insulation of electrical cables started in 1932, when Germant and Philippoff developed the simplest electrical representation of a defect within the insulation [8]. Research, over the years, lead to the improvement of this original model. The simulations discussed in this paper will be based on this well-known three-capacitor model. The first simulation model will be designed with only the basic parameters required to simulate the occurrence of discharge activity within the insulation material of an electrical cable. The simplicity of this model will cause a lack in accuracy and will also prevent the investigation of certain specific PD

characteristics. This led to the derivation of a more comprehensive simulation model.

It is essential that both models are able to accurately simulate PD activity within medium voltage cables. The chosen parameters of the simulation models are therefore very important and careful consideration is taken before choosing the simulation parameters. Cross-linked polyethylene (XLPE) has become the globally preferred insulation material for medium voltage electrical cables. This is due to the many advantages of XLPE, including: improved impact strength, dimensional stability, tensile strength and an improved resistance to aging [9]. For this reason XLPE will be used as the insulation material for both simulation models. PD in electrical cables generally occurs due to cavities within the insulation material of the cable [10]. Both models simulate PD activity due to a single void within the insulation material of an electrical cable. The dimensions of the void also play an essential part in assuring the accuracy of the simulation models. Voids within XLPE insulation typically have a volume of 10 mm^3, with a radius between 1 mm and 2 mm and a height between 2 mm and 3 mm [11]. This was considered when the dimensions of the voids, for both simulation models, were chosen.

3.2 Basic three-capacitor model

The type of void will have a unique effect on the PD characteristics and will therefore be the main focus of the basic three-capacitor simulation model. The chosen void parameters are also the most important factors for PD characterization. A capacitor circuit was used to model the insulation material as well as the void for the basic simulation model. The capacitor configuration shown in Figure 5 illustrates the three "zones" of the simulation model, including: the void, the insulation in the vicinity of the void and the rest of the healthy insulation [12].

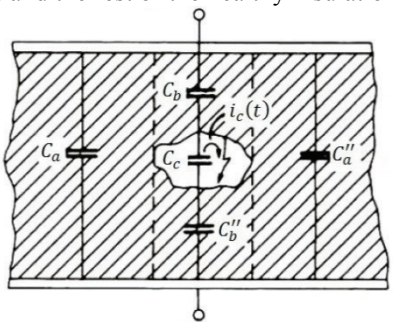

Figure 5: Capacitor configuration for basic model [12]

The derived capacitor circuit was used to design a simulation model in the Simulink® environment of MATALB®. The electrical circuit, on which the Simulink model is based, is illustrated in Figure 6. The main component of the simulation model is the capacitor configuration consisting of the three capacitors, (C_c), (C_b) and (C_a). The parallel RLC branch in the circuit will act as the input impedance to which the measuring equipment will be connected. A high voltage filter (Z) is added to the circuit for the reduction of background noise.

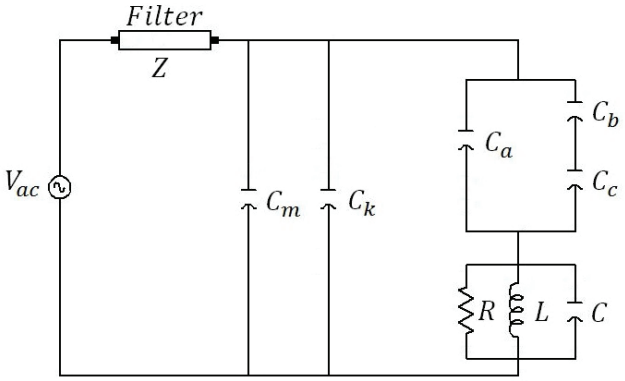

Figure 6: Derived circuit for the basic simulation model

The equations for the three capacitors of the basic simulation model will only be influenced by the permittivity of the insulation material (ε_r), the permittivity of free space (ε_0) and the dimensions of the void. The capacitance value of the capacitor associated with the void is given by [12]:

$$C_c = \frac{\varepsilon_0 \times r^2 \times \pi}{h} \tag{1}$$

The capacitance values for the healthy part of the insulation and the part of the insulation material in the vicinity of the void is calculated by means of the following two equations [12]:

$$C_a = \frac{\varepsilon_0 \times \varepsilon_r \times (a - 2b) \times b}{c} \tag{2}$$

$$C_b = \frac{\varepsilon_0 \times \varepsilon_r \times r^2 \times \pi}{h} \tag{3}$$

These three equations were used to determine the values for the capacitors required for the simulation of PD by means of the basic three-capacitor simulation model.

The first set of simulations was performed in order to study the effect of the input voltage on the maximum amplitude of the measured PD signal. The input voltage was incremented from 7 kV to 50 kV with a constant void size. The results from these simulations are depicted in the graph shown in Figure 7.

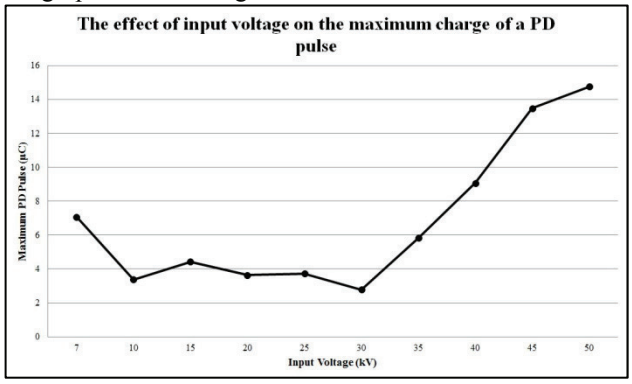

Figure 7: Effect of input voltage on the maximum PD amplitude

From the graph it can be seen that the resulting PD magnitudes, for input voltage between 10 kV and 30 kV, varies between 2 μV and 5 μV. An unusual high maximum PD amplitude is present at an input voltage of 7 kV. The conclusion can be made that the maximum PD amplitude will remain relatively constant for a range of input values. As the input voltage is increased beyond the 30 kV mark, the maximum amplitude also increases. It can therefore be said that an increase in input voltage will result in increased maximum amplitudes of the measured PD signal.

The correlation between the void size and the determined apparent charge was also investigated by means of a set of simulations. The void dimensions included a constant height of 3 mm and the radius of the void was incremented in sizes of 0.5 mm from 1 mm to 5 mm. The input voltage was kept at a constant value for all of the simulations. The change in void parameters for each simulation will result in different capacitance values of the test object. Equations (1), (2) and (3), were used to determine the capacitors of the test object for each of the simulations. The results of this set of simulations are shown in Figure 8.

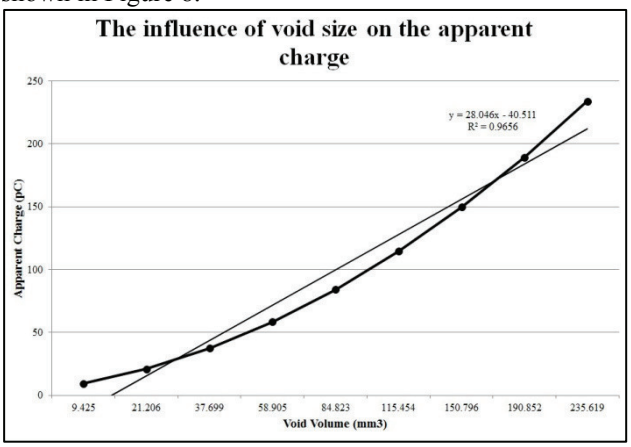

Figure 8: Correlation between void size and apparent charge

A study of the results shown in the graph led to the conclusion that, the correlation between void size and apparent charge is almost linear. A trendline was fitted to the data to be able to determine the coefficient of determination (R^2). The determined coefficient of determination was $R^2 = 0.9656$. The R^2 value indicates that the trendline is a close representation of the actual data. From this the conclusion can be made that a larger void volume will result in an almost linear increase in calculated apparent charge values; this will then result in more severe PD activity within the cable. The equation of the trendline, $y = 28.046x - 40.511$, can be used with the calculated apparent charge value to determine an estimate void size.

The basic three-capacitor simulation model was also used to study the effect of the input frequency on the apparent charge of the PD signal. The results are shown in Figure 9.

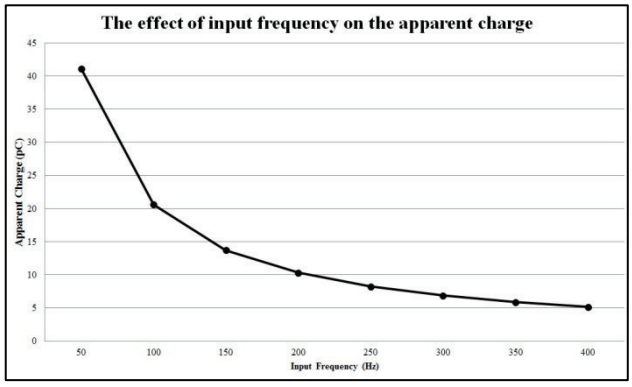

Figure 9: The effect of input frequency on the apparent charge

Published research showed that there is no trend in the effect of input frequencies below 50 Hz on PD characteristics [13]. Input frequencies between 50 Hz and 400 Hz were therefore used for this set of simulations. From the graph it is clear that the input frequency has a definite effect on the apparent charge of the measured signal. As the input frequency is increased above the normal operating frequency of 50 Hz, the apparent charge will decrease. The input frequency will also have an effect on other PD characteristics, such as: PD inception voltage, PD signal magnitude and rise and fall times [13].

3.3 Comprehensive simulation model

The comprehensive simulation model is an improvement of the basic simulation model and will therefore be based on the same principles. The improvements of the comprehensive model resulted in a more complex simulation model. Figure 11 shows the cross sectional view of the basic structure of a medium voltage electrical cable [14].

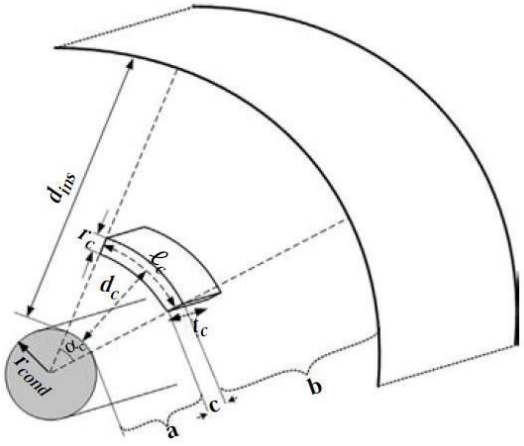

Figure 11: Capacitor configuration comprehensive simulation model [14]

The model shown in Figure 11 was used to derive an electrical circuit which was used to perform the simulations associated with the comprehensive three-capacitor model.

The electrical circuit which was used to create the Simulink® model for the comprehensive simulations is shown in Figure 12.

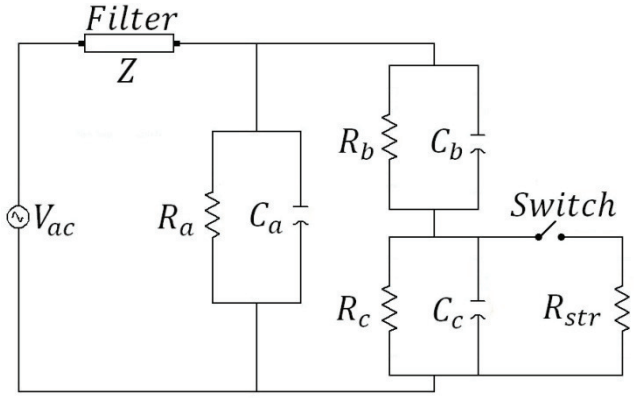

Figure 12: Derived circuit for the basic three-capacitor simulation model

It is clear that the circuit used for the comprehensive simulations has distinct similarities to the circuit used for the basic simulations. The void capacitor is denoted by (C_c), the capacitor of the insulation in the vicinity of the void by (C_s) and the capacitor of the healthy insulation by (C_p). The improvements of the comprehensive model led to the addition of resistors associated with each of the capacitors of the test object. The void resistor is given by (R_c), the resistor for the insulation in the vicinity of the void by (R_s) and the resistor for the rest of the healthy insulation by (R_p). The streamer resistance of the circuit is denoted by (R_{str}). A voltage controlled switch was used to initiate the occurrence of PD activity for this simulation model.

The insulation in the vicinity of the void is divided into two parts, "a" and "b", the capacitor values for both parts are calculated by means of the following equations [14]:

$$C_a = \frac{\varepsilon_{ins}}{\ln\left(\left(r_{cond} + d_c - {}^{r_c}/_2\right)/r_{cond}\right)} \cdot \frac{l_c}{(r_{cond} + d_c)} \cdot t_c \quad (4)$$

$$C_b = \frac{\varepsilon_{ins}}{\ln\left((r_{cond} + d_{ins})/(r_{cond} + d_c + {}^{r_c}/_2)\right)} \cdot \frac{l_c}{(r_{cond} + d_c)} \cdot t_c \quad (5)$$

The capacitance value for the insulation in the vicinity of the void is calculated by means of equation (4) and equation (5) as the equivalent series capacitance value of (C_a) and (C_b):

$$C_s = \frac{C_a C_b}{C_a + C_b} \quad (6)$$

The resistance of part "a" and part "b" of the insulation can be determined by means of the following derived equations [14]:

$$R_a = \frac{1}{\sigma_{ins}} \cdot \frac{r_{cond} + d_c}{l_c t_c} \cdot \ln\left(\frac{r_{cond} + d_c - r_c/2}{r_{cond}}\right) \quad (7)$$

$$R_b = \frac{1}{\sigma_{ins}} \cdot \frac{r_{cond} + d_c}{l_c t_c} \cdot \ln\left(\frac{r_{cond} + d_{ins}}{r_{cond} + d_c + r_c/2}\right) \quad (8)$$

The resistance value for the insulation material in the vicinity of the void is found by means of the equivalent series resistance value of (R_a) and (R_b):

$$R_s = R_a + R_b \quad (9)$$

The capacitance value for the rest of the healthy insulation is calculated by means of the following equation [14]:

$$C_p = \frac{2\pi\varepsilon_{ins}}{\ln((r_{cond} + d_{ins})/r_{cond})} \cdot L \quad (10)$$

The resistance value for this part of the insulation can be found by means of similar assumptions used to determine the value of (C_p) [14]:

$$R_p = \frac{1}{2\pi L\sigma_{ins}} \cdot ln\left(\frac{r_{cond} + d_{ins}}{r_{cond}}\right) \quad (11)$$

The capacitance value of the capacitor associated with the void is determined with the following equation [14]:

$$C_c = \frac{\varepsilon_0}{\ln\left((r_{cond} + d_c + {}^{r_c}/_2)/(r_{cond} + d_c - {}^{r_c}/_2)\right)} \cdot \frac{l_c}{(r_{cond} + d_c)} \cdot t_c \quad (12)$$

The resistance value of the resistor associated with the void is then determined by means of:

$$R_c = \frac{1}{\sigma_c} \frac{r_{cond} + d_c}{l_c t_c} \ln\left(\frac{r_{cond} + d_c + r_c/2}{r_{cond} + d_c - r_c/2}\right) \quad (13)$$

The first set of simulations performed by means of the comprehensive simulation model was used to study the effect of the input voltage on the apparent charge of the PD signal. For this set of simulations the void size was kept constant and the input voltage was incremented by 0.5 kV from 6.6 kV to the final value of 11 kV. The results are shown in Figure 13

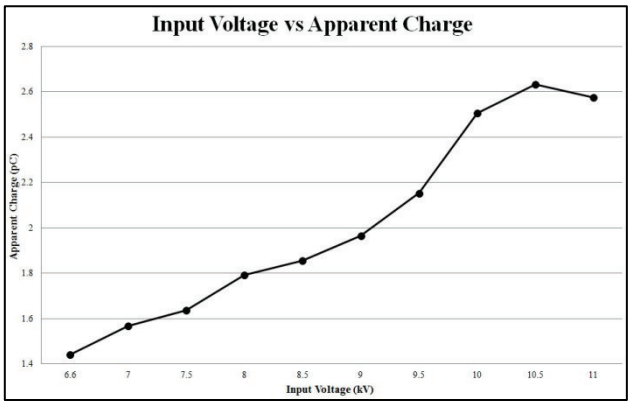

Figure 13: Correlation between input voltage and apparent charge

From Figure 13 it can be seen that an increase in input voltage will result in increased values for the apparent charge. There is however no direct trend between these two parameter. The basic simulation model as well as published work from other researchers yielded similar results.

The comprehensive model can be used to study the effect of both void size and position on the apparent charge. Three different void positions with the exact same void volume were used for this investigation. The three positions included: 1) a void in the middle of the insulation, 2) a void close to the conductor as well as 3) a void near the sheath of the cable. The following equations were used to calculate the position of each void [14]:
Close to the conductor:

$$d_c = 0.15 d_{ins} \quad (14)$$

Middle of insulation:

$$d_c = 0.5 d_{ins} \quad (15)$$

Near the sheath:

$$d_c = 0.85 d_{ins} \quad (16)$$

The length of the void (l_c) was incremented from 1 mm to 5 mm while both the height (r_c) and width (t_c) were kept constant. The simulations for all three the void positions were conducted and the results obtained from each set of simulations were used to draw a graph to show the effect of void volume and void positions on the same graph. The results are shown in Figure 14.

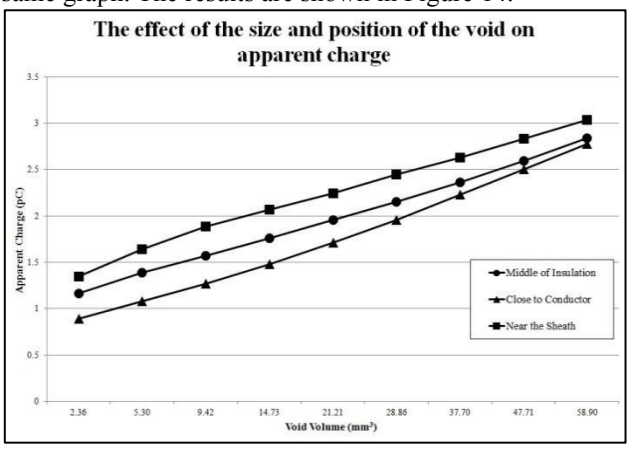

Figure 14: Effect of void parameters on the apparent charge

The graphs in Figure 14 show that an increased void volume will result in an increased value for the calculated apparent charge of the PD signal. The results obtained by means of the basic simulation model were similar to the results obtained from the comprehensive model. The coefficients of determination for the three positions are: middle of the insulation R^2 = 0.9983, close to the conductor R^2 = 0.9943 and near the outer sheath of the cable R^2 = 0.9958. It is thus confirmed that an increased void volume will result in an almost linear increase in apparent charge of the PD signal. The position of the void has an influence on the amplitude of the apparent charge.

The simulations discussed in this paper were used to investigate the effect of a variety of parameters on PD characteristics. The results obtained from both the basic and the comprehensive simulation models show similarities when compared. Results obtained from published research were also compared to the simulation results discussed in this paper. The similarities between results from published research and the results discussed in this paper verify the validity of the simulation models.

4. EXPERIMENTAL SETUP AND RESULTS

4.1 Introduction

The designed CM technique discussed in Section 2 of this paper was used to measure and analyse practical PD data. The experimental setup as well as the analysis of the measured data will be discussed in this section. The purpose of the designed CM technique is only to detect the presence of discharge activity within medium voltage cables and to analyse the measured PD data to some extent. It is necessary to utilize a number of CM techniques as well as the expertise of a specialist for the complete analysis of PD data. The complete CM technique can be divided into a number of stages which must be completed in order to be able to detect the presence of PD within the insulation material of electrical cables. A functional flow diagram of the required steps is illustrated in Figure 15.

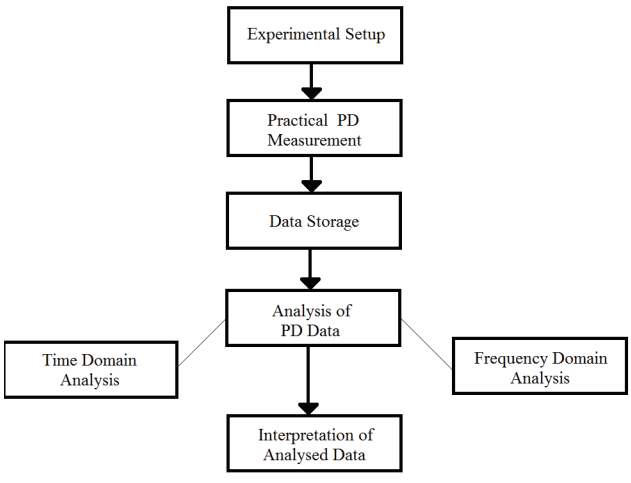

Figure 15: Flow diagram of the stages for the CM technique

The first stage of the CM technique includes the experimental setup of measuring equipment and the test specimen. The next stage is to perform accurate PD measurements on the test specimen. The data obtained from the measurements is then stored for analysis. MATLAB® programs are used to analyse the PD data in the time- and frequency-domain. The final step of the CM technique is to interpret the analysed data. This is the most important step of the entire process and is also the part where the expertise of a specialist is required for the correct interpretation of analysed PD data.

4.2 Experimental setup

The experimental setup of the CM technique includes the combination of measuring equipment and test specimen required for the measuring of practical PD data. The experimental setup of the measuring equipment is shown in Figure 16.

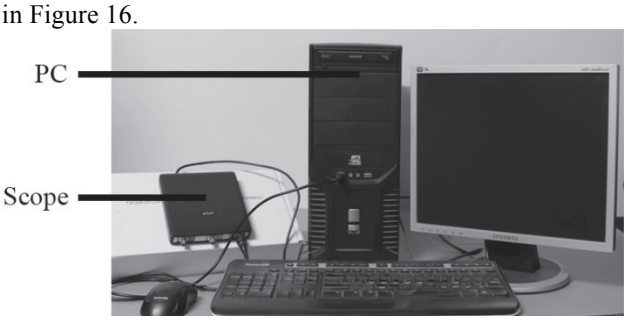

Figure 16: Experimental setup of measuring equipment

The measuring equipment includes a PC, used to control the system as well as to act as storage device for the measured data, and the digital oscilloscope which acts as the data acquisition unit of the CM technique.

A cable termination was used as the test specimen for the measurement of practical PD data. The cable termination was taken out of operation due to the fact that severe levels of discharge activity were detected within this section of the cable. The test specimen is shown in Figure 17.

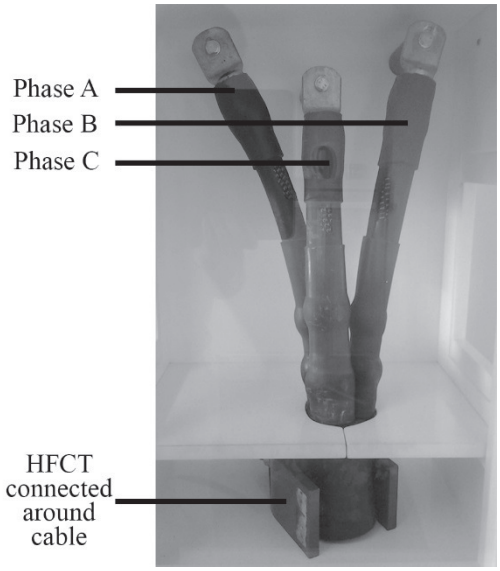

Figure 17: Cable termination

The connection of an HFCT around the cable can be seen in Figure 17. The cable termination is connected to a high voltage variac for the supply of variable input voltages. Sets of measurements were taken at input voltages of 1.6 kV, 3.2 kV and 5 kV. The different levels of input voltage facilitate the study of the effect of input voltage on PD characteristics.

5.3 Analysis of PD data

The process of measuring PD data can be seen as a relatively easy process to perform. The analysis of the measured data is however far more difficult. Modern CM techniques can be used to analyse measured PD data to some extent, but CM techniques are still dependent on the expertise of a specialist for successful analysis of the condition of electrical equipment.

The HS5 scope was used to store the measured data in ".mat" files, which can be accessed by the designed MATLAB® programs. The time domain analysis of the measured data includes: the study of the PD signal over time, the calculation of maximum and average PD amplitude, the calculation of the amount of discharges per phase as well as the ability to indicate the phase patterns of discharges. The time domain program was used to store and analyse data for three cycles (60 ms) of the input voltage. The graphical user interface (GUI) for the designed time domain MATALAB® program is shown in Figure 18.

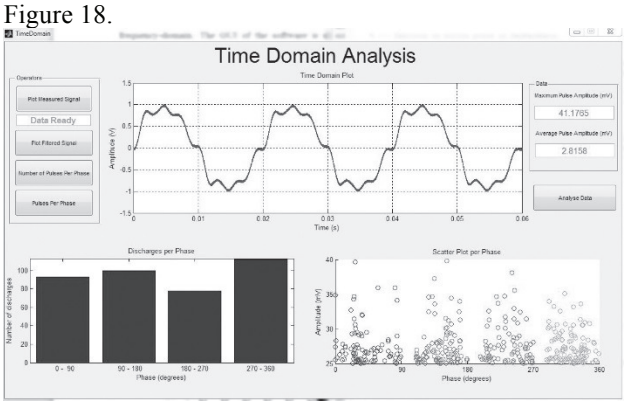

Figure 18: Time domain GUI of MATLAB program

The function to determine the number of discharges per phase was used to analyse the measured data. The results obtained from this function are given in Table 2.

Table 2: Amount of PD pulses per phase

Input voltage (kV)	First phase	Second phase	Third phase	Fourth phase
1.6	93	100	78	112
3.2	140	189	137	214
5	274	356	218	365

The numerical values were also used to construct a histogram of the results in order to be able to study the correlation between the input voltage and the number of discharges per phase. The histogram is shown in Figure 19.

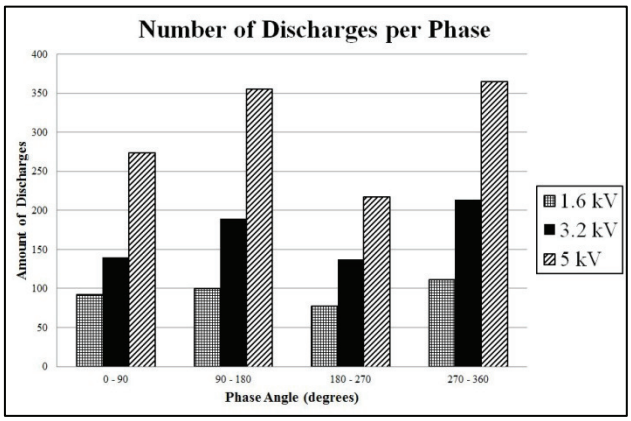

Figure 19: Histogram of amount of PD pulses per phase

From this graph it can be seen that a common trend for all the input voltages are present. The conclusion was made that an increased input voltage will result in increased amounts of discharges per phase. This trend is also present in the results obtained from the simulation models. The graph shows a significant increase in the number of discharges per phase at the 5 kV input voltage. This can be a result of the level of degradation of the cable being tested. When the 5 kV level is reached the input voltage is at such a level that PD activity reaches a critical level and will therefore cause a significant increase in various PD characteristics.

The phase pattern of the measured PD data is shown in Figure 20. The obtained PD patterns are compared to characteristic PD patterns in order to perform PRPD analysis of the measured data.

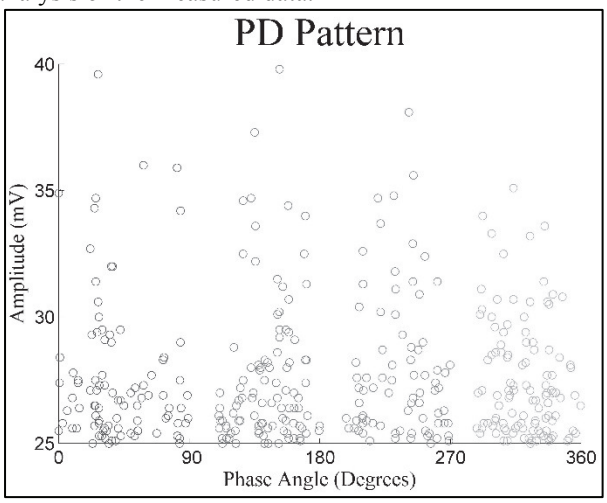

Figure 20: Phase plot of PD patterns at 1.6 kV

The plot shown in Figure 20 was compared to published research as well as characteristic PD patterns to be able to determine the types of discharges present within the test specimen. By means of comparison to the work of Hudon and Bélec [15], it was determined that both internal PD as well as exciter pulses is present within the test specimen. The measurements were taken up to a maximum bandwidth of 50 MHz; it is possible that other PD patterns may be visible if data samples are taken above the 50 MHz bandwidth. PD patterns may be clearer if more samples are taken at each measurement. The reason for this is that insufficient samples may not be enough to reveal a recognizable pattern.

The most important part of the frequency domain analysis is the ability to perform FFT analysis of the recorded time domain signals. The GUI for the frequency domain MATALAB® program is illustrated in Figure 21

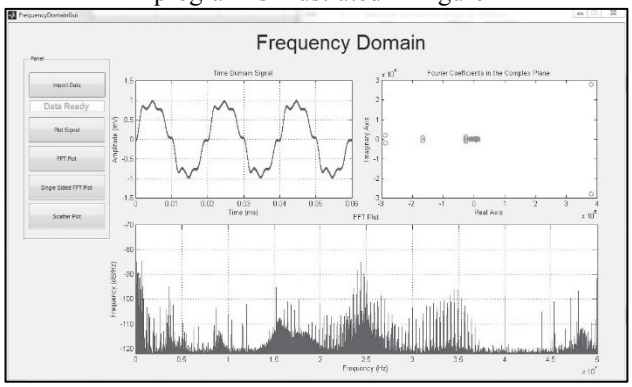

Figure 21: Frequency domain GUI of the MATLAB program

The FFT function is an algorithm which is used to compute the DFT of time domain data. The DFT is a useful operation, but computing it directly from the definition can be a time consuming operation. An FFT is used to compute the same result, but with improved speed. The FFT plot of the measured signal, at 1.6 kV, is shown in Figure 22.

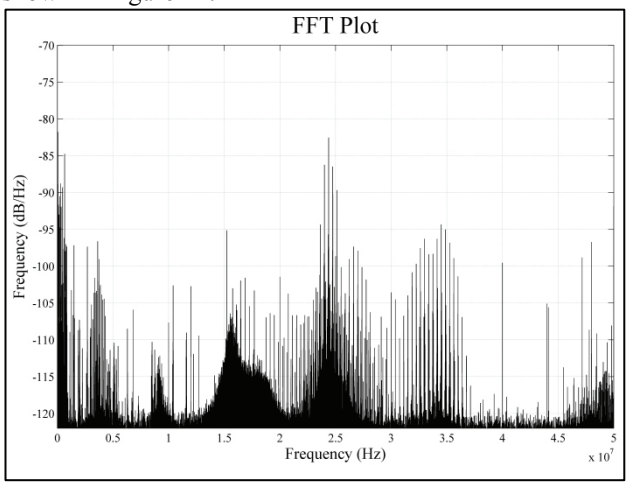

Figure 22: FFT plot at 1.6 kV

Frequency analysis of PD data associated with electrical cables is often used to determine the location of the discharge activity. The FFT plot shown in Figure 22 shows that the discharges are spread over the entire frequency range. A large portion of the discharges are however present between 15 MHz and 35 MHz. The fact that discharges are present in large portions of the measured frequency range testifies to the severity of the measured discharge activity. If the severity of PD activity within a power cable increases to reach a high level, the pulses shown in the FFT plot will continue to grow until most of the frequency range is covered.

5. CONCLUSION

A CM technique was designed which can be used to monitor the condition of electrical cables by means of PD measurements. The CM technique consists of: a sensor, a data acquisition unit and a PC. The type of sensor used for this technique is an HFCT with a physical structure representing a horseshoe. The use of an HFCT as the sensor ensures the safety of this technique, due to the fact that the measuring equipment is isolated from the typically high operating voltages. The data acquisition unit of this technique was a digital oscilloscope. The Handyscope HS5 was chosen due to a number of advantages of this scope. The final component of the CM technique is the PC. The PC is used to control the system and also to act as storage device for measured PD data. Two MATLAB® programs were designed to perform the analysis of measured PD data in both the time- and frequency-domain.

Simulation models were used to simulate the occurrence of PD activity within medium voltage electrical cables. The PD activity is due to a single void within the insulation material of the cable. Research indicated that the well-known three-capacitor model is commonly used to derive mathematical models for the representation of PD activity. The basic three-capacitor simulation model was derived with only the basic required parameters to be able to simulate PD activity. The simplistic approach of this model led to the inability to investigate the effects of a variety of parameters on the PD characteristics. This and reduced accuracy were the main reasons for the development of a more comprehensive model. The comprehensive model is able to investigate a number of crucial PD parameters. The comprehensive model also includes the stochastic nature of PD. The results obtained from the simulations discussed in this paper were used to gain knowledge regarding the phenomenon known as PD.

The designed CM technique was used to measure practical PD data. The test specimen used for the experimental results was a cable termination, taken out of operation due to the fact that discharge activity was previously detected in this component. The measured data was analysed in the time domain in order to determine: the maximum and average amplitudes of the recorded signal, the amount of discharges per phase as well as to plot the phase patterns of the PD pulses. The phase patterns are used to perform PRPD analysis of the measured PD data. This is done by comparing the obtained patterns to characteristic PD patterns as well as patterns of published research. The frequency domain program is used to analyse the measured time domain data in the frequency domain. An FFT function is used to convert the time domain data to the frequency domain. The FFT plots of the measured data were used to investigate: the frequencies at which the discharge activity is most prolific and the severity of the discharge activity.

6. REFERENCES

[1] M. Villaran and R. Lofaro, *Essential Elements of an Electric Cable Condition Monitoring Program*, 1st ed. Upton, NY: Brookhaven National Laboratory, 2010.

[2] A. Haddad and D. Warne, *Advances in High Voltage Engineering*. London, UK: Institution of Electrical Engineering, London, 2004, ch. 4, pp. 139-185

[3] S. Chaikin, "Partial Discharge Testing - Decreasing the Field Failures of High Voltage Components," *HT LLC*, pp. 1-18, March 2001.

[4] Y. Song and Y.H. Han, "Condition Monitoring Techniques for Electrical Equipment - A Literature Survey," *IEEE Transactions on Power Delivery*, vol. 18, no. 1, pp. 4 - 13, January 2003.

[5] Brookhaven National Laboratory, "Assessment of Environmental Qualification Practices and Condition Monitoring Techniques for Low-Voltage Electric Cables," vol. 2, no. 1, February 2001.

[6] IEEE Standards, "IEEE Guide for Field Testing and Evaluation of the Insulation of Shielded Power Cable Systems," IEEE Power Engineering Society, New York, NY, Standard 400, 2001.

[7] Techimp. (2013, June) Techimp Systems. [Online]. http://www.techimp.com/systems/Products/Sensors/PDSensors.aspx

[8] D.A. Nattrass, "Partial discharge XVII The early history of partial discharge research," *IEEE Electrical Insulation Magazine*, vol. 9, no. 4, 1993.

[9] I. A. Metwally, "High-voltage power cables plug into the future," *Potentials, IEEE*, vol. 27, no. 1, pp. 18 - 25, Jan - Feb 2008.

[10] N. Ahmed and N. Srinivas, "Partial Discharge Severity Assessment in Cable Systems," in *Transmission and Distribution Conference and Exposition*, 2001, pp. 849 - 852.

[11] C.Y. Ren, Y.H. Cheng, P. Yan, Y.H. Sun, and T. Shao, "Simulation of Partial Discharge in Single and Double Voids Using SIMULINK," in *Twenty-Seventh International Conference Record of the Power Modulator Symposium*, May 2006, pp. 120-123.

[12] A. Sabat and S. Karmakar, "Simulation of Partial Discharge in High Voltage Power Equipment," *International Journal on Electrical Engineering and Informatics*, vol. 3, no. 1, pp. 234-247, 2011.

[13] C. Nyamupangedengu and I.R. Jandrell, "Partial Discharge Spectral Response to Variations in the Supply Voltage Frequency," *IEEE Transactions on Dielectrics and Electrical Insulation*, vol. 19, no. 2, pp. 521 -531, April 2012.

[14] F Haghjoo, E Khanahmadloo, and S.M. Shahrtash, "Comprehensive 3-capacitor model for partial discharge in power cables," *COMPEL: The International Journal for Computation and Mathematics in Electrical and Electronic Engineering*, vol. 31, no. 2, pp. 346 - 368, 2012.

[15] C. Hudon and M. Bélec, "The Importance of Phase Resolved Partial Discharge Pattern Recognition for On-Line Generator Monitoring," in *IEEE International Symposium on Electrical Insulation*, Arlignton, Virginia, USA, June 1998, pp. 296 - 300.